Vol 18 No 7, July 2009
1674-1056/2009/18(07)/2703-06

Chinese Physics B

© 2009 Chin. Phys. Soc.
and IOP Publishing Ltd

Dynamic characteristics and simulation of traffic flow with slope*

He Hong-Di(何红弟)[a], Lu Wei-Zhen(卢伟真)[a]†, Xue Yu(薛 郁)[b], and Dong Li-Yun(董力耘)[c]

[a] *Department of Building and Construction, City University of Hong Kong, Hong Kong, China*
[b] *Department of Physical, University of Guang Xi, Nanning* 530004, *China*
[c] *Shanghai Institute of Applied Mathematics and Mechanics, Shanghai University, Shanghai* 200072, *China*

(Received 26 September 2008; revised manuscript received 18 December 2008)

This paper proposes a new traffic model to describe traffic flow with slope under consideration of the gravity effect. Based on the model, stability analysis is conducted and a numerical simulation is performed to explore the characteristics of the traffic flow with slope. The result shows that the perturbation of the system is an inherent one, which is induced by the slope. In addition, the hysteresis loop is represented through plotting the figure of velocity against headway and highly depends on the slope angle. The kinematic wave at high density is also obtained through reproducing the phenomenon of stop-and-go traffic, which is significant to explore the phase transition of traffic flow and the evolution of traffic congestion.

Keywords: traffic flow, perturbation, stability analysis, slope
PACC: 0550, 6470

1. Introduction

In the last decade, traffic problems have attracted considerable attention in many metropolitan cities. Scholars and engineers have developed many traffic models such as the car-following model, the cellular automaton model, the gas kinetic model and the hydrodynamic model. They all provide us with a good understanding of stop-and-go traffic from different points of view. Among these, the car-following model, which describes the interaction of two successive cars from the microscopic view, has been extensively applied to investigate the characteristics of traffic flow in many aspects.[1−12]

The car-following model is developed to represent the motion of vehicles following each other on a single lane without any overtaking. It is based on the assumption that each driver reacts in some specific fashion to a stimulus from the vehicle ahead of him. Reuschel[1] and Pipes[2] were pioneers in the development of the traffic model in the early 1950s. Based on their works, many advanced car-following models were proposed by scholars such as Chadler, Newell, Edie, Gazies, *et al.*[3−6] In these classical car-following models, each vehicle obeys the common equation of motion, which is determined by the relation of other cars moving in the traffic flow. Some traffic phenomena could be illustrated from these models and these also enable us to establish a bridge between the microscopic and the macroscopic views. One of the most impressive models is the optimal velocity model (OPV), which was presented by Bando *et al* in 1995.[7] It is based on the idea that each vehicle has an optimal velocity, which depends on the following distance of the preceding vehicle. Applying the OPV, one can describe many properties of real traffic flows, such as the instability of traffic flow, the evolution of traffic congestion and the formation of stop-and-go waves.[8−18]

These models, however, are only suitable to describe the traffic flow in the flat landform. The special landform such as a harbor tunnel or a bridge, which is characterized with slope and results in different traffic properties, is seldom considered. Due to the special landform structure including downgrade and upgrade, the influence of gravity should not be ignored. Although Li *et al*[19] investigated the effect of the small slope on traffic flow by introducing a generalized optimal speed function to consider the slope grade, the influence of

*Project supported partially by the Strategic Research Grants from City University of Hong Kong (Grant Nos SRG 7002226(BC) and SRG 7002370(BC)), and the National Natural Science Foundation of China (Grant Nos 10662002, 10672098 and 10532020).
†Corresponding author. E-mail: bcwzlu@cityu.edu.hk

gravity is still not taken into account. In this paper, we extend the classical optimal speed model to investigate the traffic flow with slope through considering the gravity. The rest of the present paper is organized as follows. In Section 2, the slope model is introduced by taking into account the gravity effect. Stability analysis is carried out in Section 3 and numerical simulation is performed in Section 4. The last section is devoted to a summary and the prospect of further study.

2. Traffic model

The new model is extended based on the harbor tunnel which includes two various slopes, i.e., downgrade and upgrade (Fig.1). For the purpose of real application, the single-lane roadway with three flat sections linking two slopes is proposed to study the characteristics of traffic with slope under a periodic boundary condition.

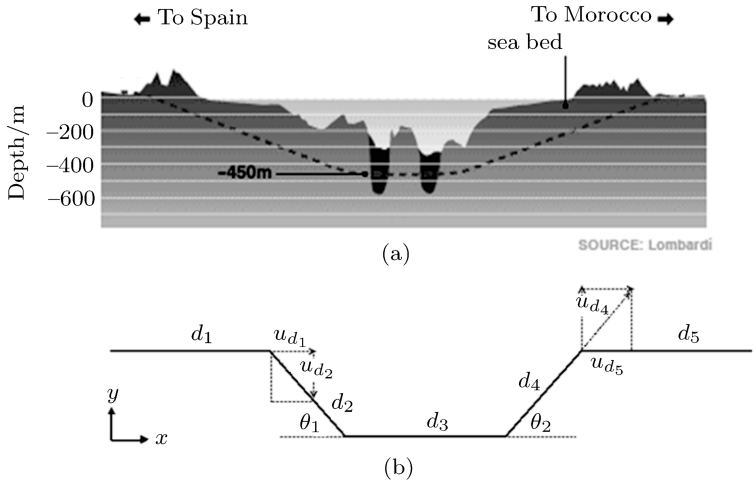


Fig.1. Cross-section and longitudinal profile of the tunnel.

Considering the gravity effect in the special landform, we propose a new traffic model based on the OPV in this study. The model is described by the following equations of vehicle movement:

$$\ddot{x}_n = a\left(V(\Delta x_n) - \dot{x}_n\right) + f(x_n),$$

$$f(x_n) = \begin{cases} 0 & 0 \le x_n < d_1, \\ g\sin\theta_1 & d_1 \le x_n < d_2, \\ 0 & d_2 \le x_n < d_3, \\ -g\sin\theta_2 & d_3 \le x_n < d_4, \\ 0 & d_4 \le x_n < d_5, \end{cases} , \qquad (1)$$

where $V(\Delta x)$ is the optimal-velocity function,$x_i(t)$ is the position of vehicle i at time t, $\Delta x_i(t) = (x_{i+1}(t) - x_i(t))$ is the headway of vehicle i at time t, and a is the sensitivity.

A driver adjusts the vehicle speed to approach the optimal velocity based on the observed headway. Sensitivity a allows for the time lag $\tau = 1/a$, and takes the vehicular velocity to reach the optimal velocity when the traffic is varying. Generally, it is necessary that the optimal velocity function has the following properties: it is a monotonically increasing function and has an upper bound (maximal velocity). The optimal velocity function of vehicles is given by

$$V(\Delta x) = \frac{v_{\max}}{2}[\tanh(\Delta x - x_s) + \tanh(x_s)], \qquad (2)$$

where $v_{\max}$ is the maximal velocity of vehicles on the roadway and x_s is the safety distance.

The effect of gravity is shown by $f(x)$, which is the function of the gravity and the slope angle. When the slope angle decreases to zero, the upgrade and the downgrade sections become flat and the model is reduced to the OPV model.

From Fig.1, the road is divided into five sections and all vehicles obey Eq.(1) with different conditions. When a vehicle just moves from one section to the next section, the velocity of the vehicle will jump to a

various value. The variation of the velocity from the d_1 to d_2 road sections can be obtained from the formation of $u_{d_2} = u_{d_1}/\cos\theta_1$. Similarly, the other changes when a vehicle moves to a new road section can be obtained analogously by forms of $u_{d_3} = u_{d_2}\cos\theta_1$, $u_{d_4} = u_{d_3}/\cos\theta_2$, $u_{d_5} = u_{d_4}\cos\theta_2$. To simulate the traffic flow in a real condition, the maximal velocity $v_{\max}$ is used for the whole road sections.

3. Stability analysis

3.1. Flat section

According to Eq.(1), the solution of steady state flow in the flat section can be easily obtained,[7]

$$x_n^{(0)} = bn + ct \tag{3}$$

with

$$b = L/N\ ,\ c = V(b), \tag{4}$$

where b is the constant spacing of two successive vehicles and c is the constant velocity of the steady state of traffic flow. Hereafter we call this solution the steady state flow without congestion, in which vehicles are uniformly distributed with identical vehicle spacing and move with the same constant velocity.

Let us investigate the stability of the state of this solution by linearizing the original nonlinear system. Assume that y_n is a small deviation from the steady state flow of identical vehicle spacing, $x_n^{(0)}$, i.e.,

$$x_n = x_n^{(0)} + y_n, \quad y_n \ll 1. \tag{5}$$

Substituting it into Eq.(1) we obtain the perturbation equations:

$$\ddot{y}_n = a\left(V'(\xi) \times \Delta y_n - \dot{y}_n\right). \tag{6}$$

Then the stability in the flat section can be obtained as

$$V'(\xi) < \frac{a}{2}. \tag{7}$$

3.2. Slope section

It is obviously that the solution of steady state flow in the slope section has been changed as

$$x'^{(0)}_n = bn + ct \tag{8}$$

with

$$b = L/N\ ,\ c = V(b) \pm g\sin\theta, \tag{9}$$

where θ is the slope angle including the downgrade and upgrade sections. The positive sign represents the vehicles in the downgrade section while the negative sign describes the vehicles in the upgrade section.

Similarly, we assume a small deviation and obtain the perturbation equation

$$\ddot{y}_n = a\left(V'(\xi) \times \Delta y_n - \dot{y}_n\right) + f(x'_n) - f(x'^{(0)}_n). \tag{10}$$

Due to the x'_n and $x'^{(0)}_n$ belonging to the same slope section, the perturbation equation is reduced to Eq.(6). Then the stability in the slope section is the same as the situation in the flat section.

3.3. Cross section

In the cross section, the nth vehicle and $(n+1)$th vehicle are located in different sections and they satisfy their own equations respectively. The perturbation equation is obtained below

$$\ddot{y}_n = a\left(V'(\xi) \times \Delta y_n - \dot{y}_n\right) + f(x'_n) - f(x_n^{(0)}). \tag{11}$$

Due to the x'_n and $x_n^{(0)}$ belonging to the different sections, Eq.(11) is changed to

$$\ddot{y}_n = a\left(V'(\xi) \times \Delta y_n - \dot{y}_n\right) \pm g\sin\theta. \tag{12}$$

In engineering, the slope angle is quite small ($\theta \approx 0 \sim 5^\circ$, $\sin\theta \approx 0 \sim 0.087 \ll 1$).[17] In addition, the safety distance in the real traffic is set to $x_s = 100$ m while in the simulation it is generally set to $x_s = 2$.[9] According to this shrink relationship, all parameters in this simulation are dimensionless and the gravity is then set to $g' = 0.196 \approx 0.2$. Hence, the term of $g\sin\theta \approx 0 \sim 0.0174$ becomes quite small and the Eq.(12) can be reduced to

$$\ddot{y}_n \approx a\left(V'(\xi) \times \Delta y_n - \dot{y}_n\right). \tag{13}$$

Therefore, the stability in the cross section is nearly the same as that in the above two situations. Moreover, the phase diagram of sensitivity against headway (Fig.2) is obtained by numerical simulation of Eq.(1). From the figure, two facts are noted: one is that the apex of sensitivity (i.e. critical point) within a small slope angle ($\theta = \pi/36$) is nearly the same as that in the situation without slope; the other is that there does not exist a critical point as the angle increases to a large one ($\theta = \pi/9$). The unstable region enlarges with the increase of the angle. To sum up,

the slope plays a remarkable role in the stability of traffic flow.

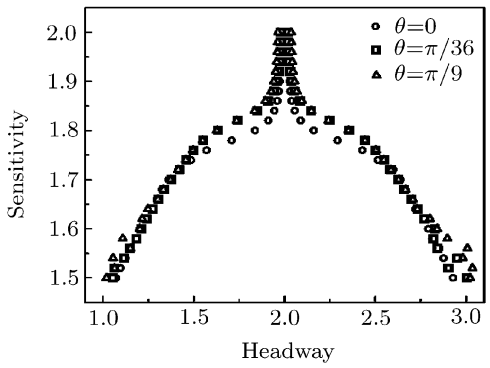


Fig.2. Phase diagram in the headway-sensitivity space for the different slope angles ($\theta = 0$ means the OPV model).

4. Results analysis of results

The simulation of the traffic flow is performed under the periodic boundary condition. We solve Eq.(1) numerically with optimal-velocity functions, i.e., Eq.(2) by using the fourth-order Runge–Kutta method where the time interval is $\Delta t = 1/100$.

The related parameters, i.e., lengths of each road sections are given as $d_1 = 100$, $d_2 = 300$, $d_3 = 800$, $d_4 = 1050$, $d_5 = 1200$. As said before, the safety distance in the real traffic is set to $x_s = 100$ m while in the simulation[9,19] it is generally set to $x_s = 2$. According to this shrink relationship, the maximum velocity is assumed to be 2 and the gravity is set to 0.2.

On a flat road section, the vehicles move smoothly with a constant velocity if the vehicles are initially located with the same headway, which has been proved by much of the literature[7−10] (Fig3(a)). Due to the slope, there appear to be four disturbances with the same initial condition (Figs.3(b)–3(d)). When a vehicle moves from one road section to another, the velocity will jump to various values, which induces a disturbance moving backward. Figures 3(b)–3(d) show the snapshots of velocity configuration of all vehicles at $t = 100$ s, 300 s and 1000 s. As the time extends, the vehicle velocities tend to locate on the two typical values, one is almost zero and the other is nearly the maximum velocity.

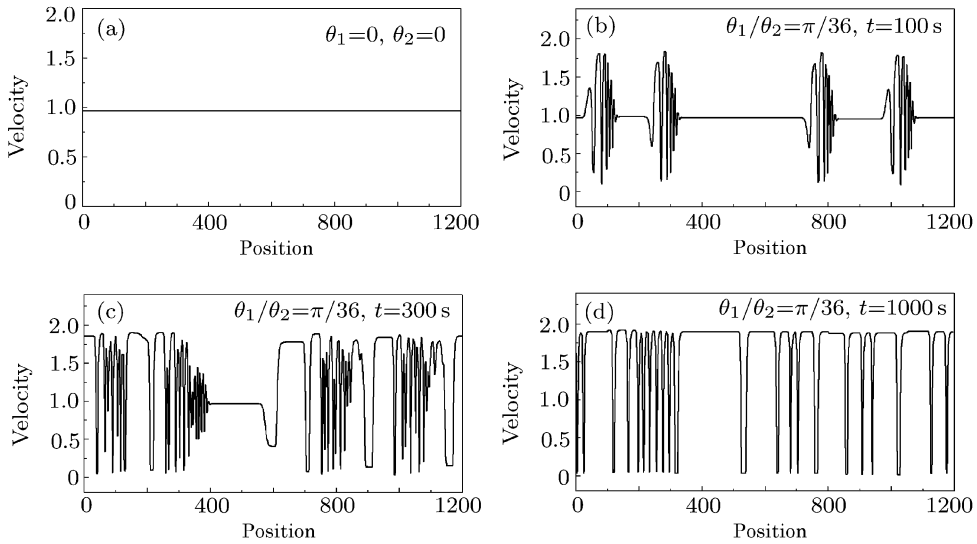


Fig.3. Velocity against position for the flat road section (a) and the road with slope sections at $t = 100$ s (b), 300 s (c) and 1000 s (d) in the unstable condition; $a = 1$, $N = 600$, $L = 1200$.

One may expect that this suggests the generation of congestion. Indeed, we can clearly observe the growth of congestion by plotting the positions of all vehicles on the circuit with time development in Fig.4. From this figure, we find that four clusters of congestion are formed from the critical location. The homogeneous flow eventually develops into congestion, which corresponds to stop-and-go

traffic. We can also observe the following process:

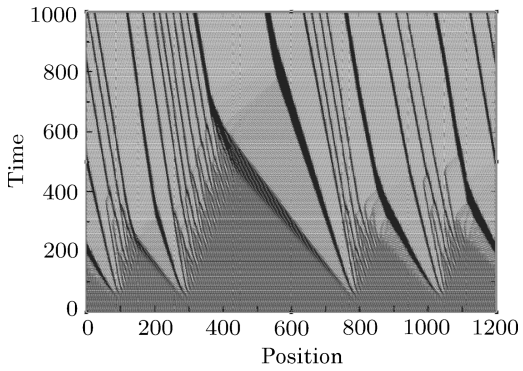


Fig.4. The spatiotemporal diagram in the unstable condition, $a = 1$, $N = 600$, $L = 1200$. The horizontal axis is the position of a car x and the vertical axis is the time t.

how the congestion structures evolve and how they move backwards respectively. The traffic jam appears as the kink-antikink density wave. Moreover, Fig.4 implies that all clusters of congestion move backwards slowly with the same velocity at last. The velocity is easily estimated by the inverse slope of the dark line, which is about 0.171.

Figure 5 shows the phase space of the velocity against the headway. When the congestion becomes stationary after enough time, the motion of vehicles organizes a 'hysteresis loop'. Comparing with the phase space in the flat road section, we know that such a 'hysteresis loop' is more complicated and slightly symmetrical. Changing the slope of the downgrade and upgrade, we find that these ranges are all changed and the symmetry breaks. Here, one point should be noted is that the slope angle plays an important role in determining the range and the symmetry of the 'hysteresis loop'.

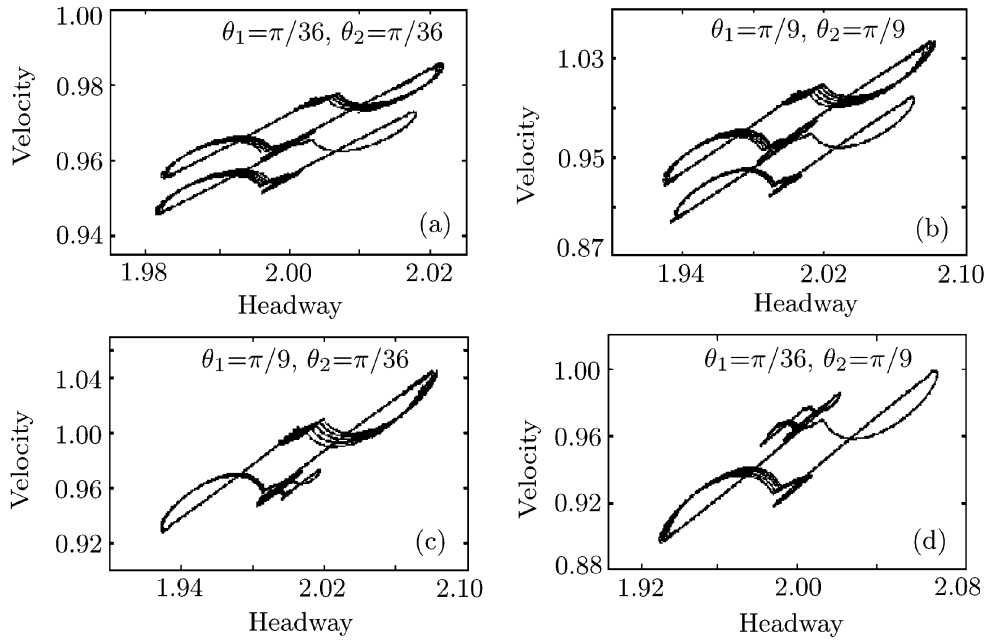


Fig.5. Hysteresis loop for the different slopes of the downgrade and upgrade $a = 2$, (a) $\theta_1 = \theta_2 = \pi/36$, (b) $\theta_1 = \theta_2 = \pi/9$, (c) $\theta_1 = \pi/9$, $\theta_2 = \pi/36$, (d) $\theta_1 = \pi/36$, $\theta_2 = \pi/9$.

In addition, we study the headway and velocity distributions accumulated over 100 seconds, respectively. Figure 6 shows the headway and velocity distributions accumulated over 100 steps. According to the refined time steps and plenty of the vehicles in this simulation, 6×10^6 vehicles are statistical for this distribution. We can read off from the final 100 steps distribution that the headway in a high concentration area, i.e., $\Delta x_{\min}$, is about 0.26 and the corresponding velocity $V(\Delta x_{\min})$ is about 0.025. On the other hand, the headway $\Delta x_{\max}$ in the low concentration area is about 3.71, in which vehicles move smoothly with velocity $V(\Delta x_{\max})$ about 1.76. If we define the congestion region as the one in which the headway of vehicles is shorter than 2 unit lengths, then the total number of vehicles in the congestion region is 300, i.e., half the total vehicles.

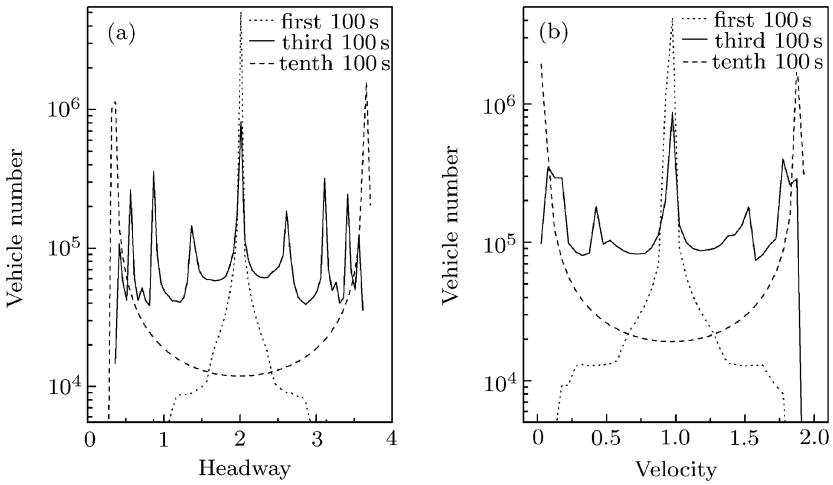


Fig.6. The headway distribution accumulated over 100 s within 10000 iteration time steps. The distributions of the first 100 s (the dotted line), the third 100 s (the solid line) and the final 100 s (the dashed line) are shown, respectively. The vertical axis displays the number of vehicles scaled in logarithm.

5. Summary

A new model which takes into account the effect of gravity is proposed to study traffic flow with slope. Stability analysis is performed and a numerical simulation is carried out to investigate the characteristics of traffic flow with slope. It can be found that the inherit perturbation emerges at the beginning of the simulation due to the existence of the slope. In addition, the phenomenon of the stop-and-go traffic is reproduced to reveal the kinematic wave speed at high density, which is significant to study the formation of congestion from an initially homogenous condition. Of course, this model is limited on the periodic boundary condition. It may be more realistic if we extend this model to the open condition, which will be investigated in future work.

References

[1] Reuschel A 1950 *Osterr. Ing. Archiv.* **4** 193
[2] Pipes L A 1953 *J. Appl. Phys.* **24** 274
[3] Chandler R E, Herman R and Montroll E W 1958 *Oper. Res.* **6** 165
[4] Newell G F 1961 *Oper. Res.* **9** 209
[5] Edie L C 1961 *Oper. Res.* **9** 66
[6] Gazis D C, Herman R and Rothery R W 1961 *Oper. Res.* **9** 545
[7] Bando M, Hasebe K, Nakayama A, Shibata A and Sugiyama Y 1995 *Phys. Rev.* E **51** 1035
[8] Bando M, Hasebe K, Nakayama A and Nakayama A 1998 *Phys. Rev.* E **58** 5429
[9] Jiang R, Wu Q S and Zhu Z J 2001 *Phys. Rev.* E **64** 017101
[10] Xue Y, Dong L Y, Yuan Y W and Dai S Q 2002 *Acta Phys. Sin.* **51** 492 (in Chinese)
[11] Hanaura H, Nagatani T and Tanaka K 2007 *Physica* A **374** 419
[12] Nagatani T 1999 *Phys. Rev.* E **60** 6395
[13] Chen X, Gao Z Y, Zhao X M and Jia B 2007 *Acta Phys. Sin.* **56** 1570 (in Chinese)
[14] Lei L, Dong L Y and Ge H X 2007 *Acta Phys. Sin.* **56** 6874 (in Chinese)
[15] Helbing D and Tilch B 1998 *Phys. Rev.* E **58** 133
[16] Mo Y L, He H D, Xue Y, Shi W and Lu W Z 2008 *Chin. Phys.* B **17** 4446
[17] Ge H X, Cheng R J and Dai S Q 2005 *Physica* A **357** 466
[18] Nagatani T 2000 *Phys. Rev.* E **61** 3564
[19] Li X L, Song T, Kuang H and Dai S Q 2008 *Chin. Phys.* B **17** 3014